Int. J. Electrochem. Sci., 13 **(2018)** 8915 – 8930, doi: 10.20964/2018.09.07

International Journal of ELECTROCHEMICAL SCIENCE
www.electrochemsci.org

Effect of Plasma Pre-oxidation on the Cu Corrosion Inhibition in 3.5% NaCl by an Environmentally Friendly Amide

N. Velazquez-Torres[1], *H. Martinez*[2], *J. Porcayo-Calderon*[1,2], *E. Vazquez-Velez*[2], *O. Florez*[2], *B. Campillo*[3], *J.G. Gonzalez-Rodriguez*[1*], *L. Martinez-Gomez*[2,4]

[1] Universidad Autonoma del Estado de Morelos, CIICAp, Av. Universidad 1001, Col. Chamilpa, 62209-Cuernavaca, Mor., Mexico
[2] Universidad Nacional Autonoma de Mexico, Instituto de Ciencias Fisicas, Av. Universidad S/N, Col. Chamilpa, 62209-Cuernavaca, Mor., Mexico.
[3] Universidad Nacional Autonoma de Mexico, Facultad de Quimica, Circuito Universitario, Mexico, D.F., Mexico
[4] Corrosion y Protección, (CyP), Buffon 46, 11590 Mexico D.F., Mexico
[*]E-mail: ggonzalez@uaem.mx

Received: 26 February 2018 / *Accepted:* 27 April 2018 / *Published:* 5 August 2018

The effect of plasma pre-oxidation on the effect of the inhibition performance of N-[2-[(2-hydroxyethyl) amino] ethyl]-amide extracted from coffee bagasse for Cu in 3.5% NaCl has been investigated by using electrochemical techniques. Electrochemical impedance spectroscopy, potentiodynamic polarization curves and linear polarization resistance (LPR) measurements were the employed techniques. Results have shown that the corrosion rate of Cu was decreased and the properties of the passive film formed by the inhibitor were improved. Corrosion protection given by the inhibitor and pre-oxidizing treatment improves as time elapses due to an increase of the surface area covered by the corrosion products layer. This has been explained in terms of a better adherence of the inhibitor-formed film to the metal which by pre-oxidizing.

Keywords: Copper, pre-oxidation, green inhibitor, corrosion.

1. INTRODUCTION

Even when Cu has a moderate uniform corrosion resistance, this is greatly reduced in environments containing ammonia, CO_2, sulfides or chlorides [1-5]. One of most widely used methods to fight corrosion is the use of organic corrosion inhibitors [6-8]. Among these, one of the most widely used are imidazolines, amides and amino acid base inhibitors [9-13]. A specific interaction between

some functional groups, which contain atoms such as nitrogen, oxygen and sulfur, due to their free and alone electron pairs, and metal surface is the main action of these inhibitors. Recently, there has been a big interest among scientific community the interest on the naturally occurring inhibitors extracted from leaves, roots and fruits because of the existence of this type of atoms contained in organic compounds [14–16] with conjugated double bonds and polar functional groups [17–20] that has been proved to efficiently inhibit copper corrosion. Some plants had been studied as corrosion inhibitors such as *Salvia officinalis* [21], *Musa paradisica* [22], *Capsicum annuum* [23], *Adhotada vasica* [24], among others. The corrosion inhibition of these plants extracts has been attributed to the presence of active principles which form protective films on metal surfaces by coordinating with metal ions through these heteroatoms. In a recent work, Porcayo-Calderon et al. [25] evaluated the use an imidazoline extracted from coffee bagasse as a green corrosion inhibitor for carbon steel in a CO_2-saturated 3.5% NaCl solution, finding it as an excellent corrosion inhibitor. The use of pre-oxidation treatment has been widely used technique to improve the high temperature oxidation and molten salt corrosion protection for metallic coatings [26-30], especially with the plasma gas oxidation technique, but its use has not been used on the corrosion inhibitors performance. Thus, the goal of this work is to evaluate the use of plasma gas pre-oxidation treatment on the corrosion inhibition performance of a naturally occurring inhibitor, namely N-[2-[(2-hydroxyethyl) amino] ethyl]-amide, extracted from coffee bagasse for Cu in a chloride-containing solution.

2. EXPERIMENTAL PROCEDURE

2.1 Testing material.

Materials used for this work was cylindrical bars of pure Cu, measuring 1.0 cm in diameter and 10 cm high. They were oxidized in a plasma gas with pure oxygen, using a pressure of 1 Torr, a voltage of 371 V and a current of 10 mA, a temperature of 600 ^{0}C during 8 hours. After this, they were encapsulated in commercial polymeric resin, ground with 1200 grade emery paper, and rinsed with acetone.

2.2 Testing solution.

As corrosive environment, a 3.5% NaCl solution was prepared by using bi-distilled water. N-[2-[(2-hydroxyethyl) amino] ethyl]-amide was used as corrosion inhibitor. Synthesis of N-[2-[(2-hydroxyethyl) amino] ethyl]-amide is described elsewhere [25]. Experiments were carried out at room temperature. Specimens were tested without pre-oxidation treatment, and pre-oxidized with the addition of 0, 5, 10, 25, 50 and 100 ppm of inhibitor. They were analyzed in a Scanning electronic microscope whereas micro chemical analysis was done with an energy dispersive of x-ray analyzer (EDX).

2.3 Electrochemical techniques.

Techniques employed in this work were electrochemical impedance spectroscopy (EIS), , linear polarization (LPR) measurements and potentiodynamic polarization curves. A flask glass cell was used for this, using a saturated calomel electrode (SCE) and a graphite rod as and auxiliary reference electrodes respectively. Electrode was hold in solution for around 20 minutes until the open circuit potential, E_{corr}, was stable, before starting the polarization curved; after that the working electrode was polarized at -500, respect to the E_{corr} value, and seep started at a constant sweep rate of 1 mV/s and the test finished when a potential +500 mV. Tafel extrapolation to calculate the corrosion current density values, I_{corr}. LPR measurements were carried out by polarizing the specimen ± 10 mV around the E_{corr} value every hour during 24 hours of testing. EIS measurements were carried out at the E_{corr} value by applying an AC signal with an amplitude of ±10 mV in the frequency range 100 kHz to 0.05 mHz.

3. RESULTS AND DISCUSSION.

3.1 Oxide characterization.

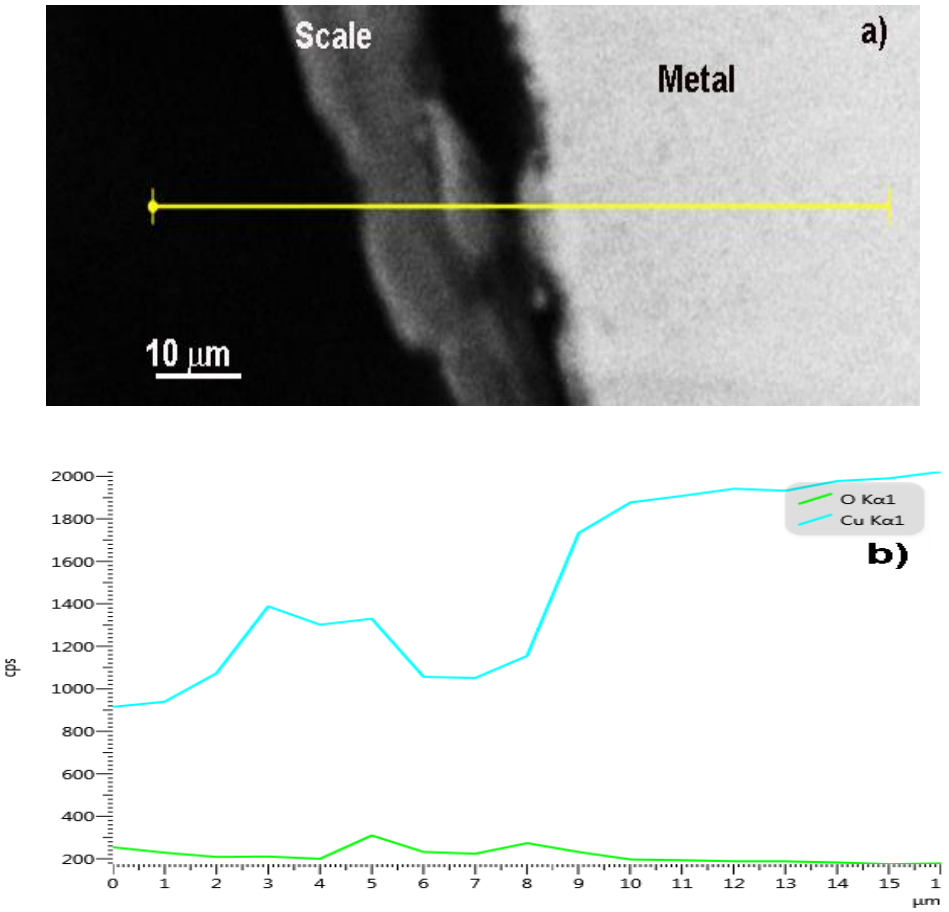

Figure 1. a) Micrograph of plasma pre-oxidized Cu, b) line-scan micro chemical analysis of the formed scale

A micrograph of a cross section of the oxidized Cu specimen is shown in Fig. 1 together with a micro chemical analysis, which shows the presence of Cu and O, which is an evidence of the presence of copper oxides on top of Cu with a thickness around 15 μm.

3.2 Open circuit potential (OCP).

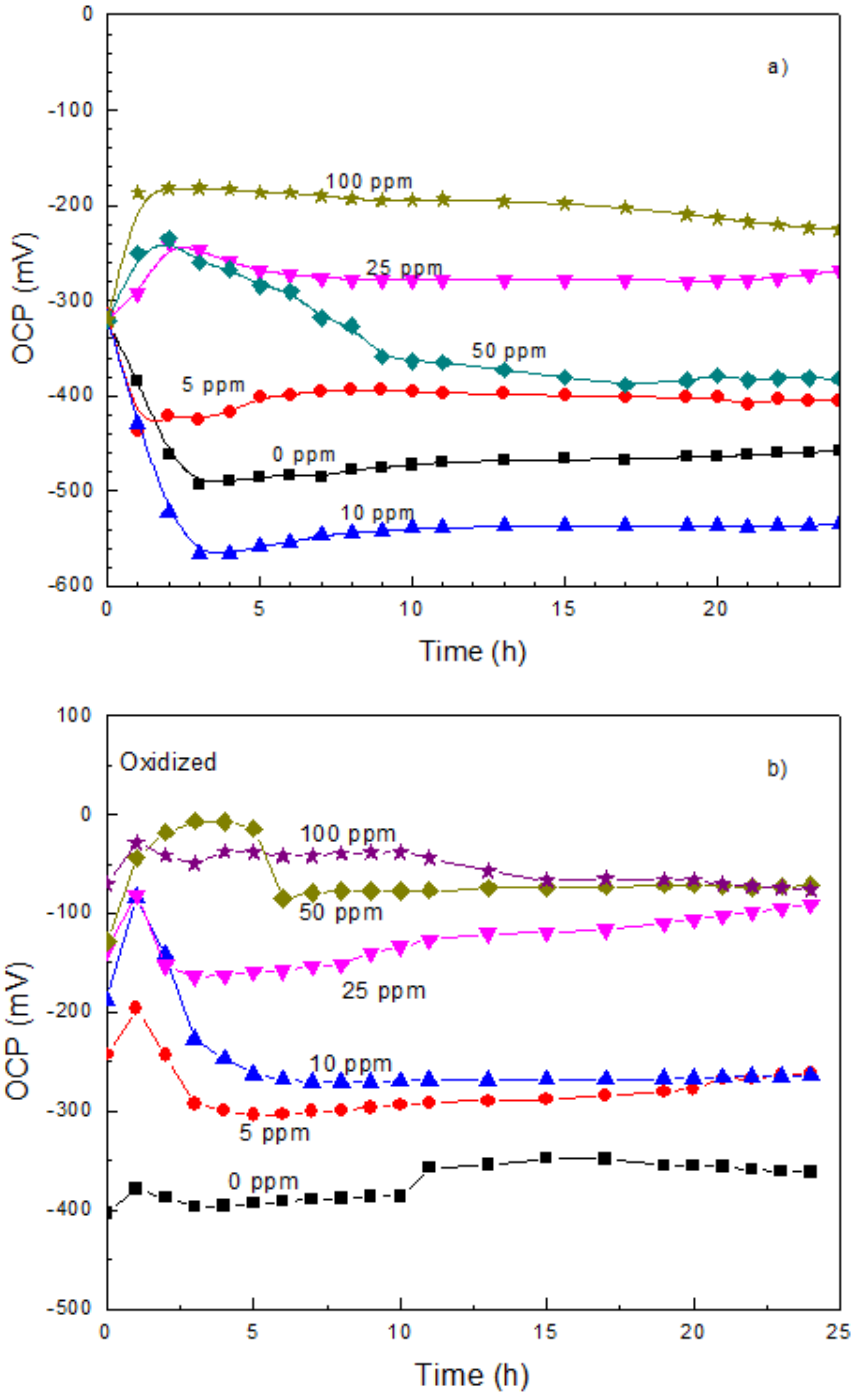

Figure 2. Effect of N-[2-[(2-hydroxyethyl) amino] ethyl]-amide concentration in the variation of the open circuit potential value (OCP) with time in 3.% NaCl for Cu specimens a) without and b) with pre-oxidizing treatment.

The variation in the Open circuit potential value (OCP) for Cu without and with pre-oxidation treatment in 3.5% NaCl solution containing different doses of N-[2-[(2-hydroxyethyl) amino] ethyl]-amide is shown in Fig. 2. It can be seen that, regardless of the presence of a pre-existing copper oxide on the metal surface, for inhibitor concentrations lower than10 ppm, Fig. 2 a, the OCP value shifts towards more active values during the first 5 hours, and remains there during the rest of the testing time. For inhibitor concentrations higher than 25 ppm, the OCP values were more positive than those obtained at lower inhibitor concentrations, but after a few hours of testing, it shifts towards more active values, except with 100 ppm, where the OCP value reached the noblest value.

However, the OCP values obtained for pre-oxidized metal were nobles than those obtained for Cu without pre-oxidation treatment, indicating a lower tendency to get corroded. The formation of a protective film on the metal surface makes the OCP value to shift towards nobler values [34], whereas the dissolution of this film makes the OCP to shift towards more negative values. In absence of inhibitor, the OCP value was nobler for pre-oxidized Cu than that obtained in absence of pre-oxidation treatment, indicating that Cu is protected against corrosion by pre-oxidizing it. Thus, the establishment of a protective film formed by the inhibitor makes the OCP value to shift towards more positive values, but later on, when this film is dissolved, OCP value is moved towards more active values. If both inhibitor and pre-formed oxide are present, they provide a much better corrosion protection to the underlying metal, making the OCP value to shift in to the noble direction.

3.3 Polarization curves.

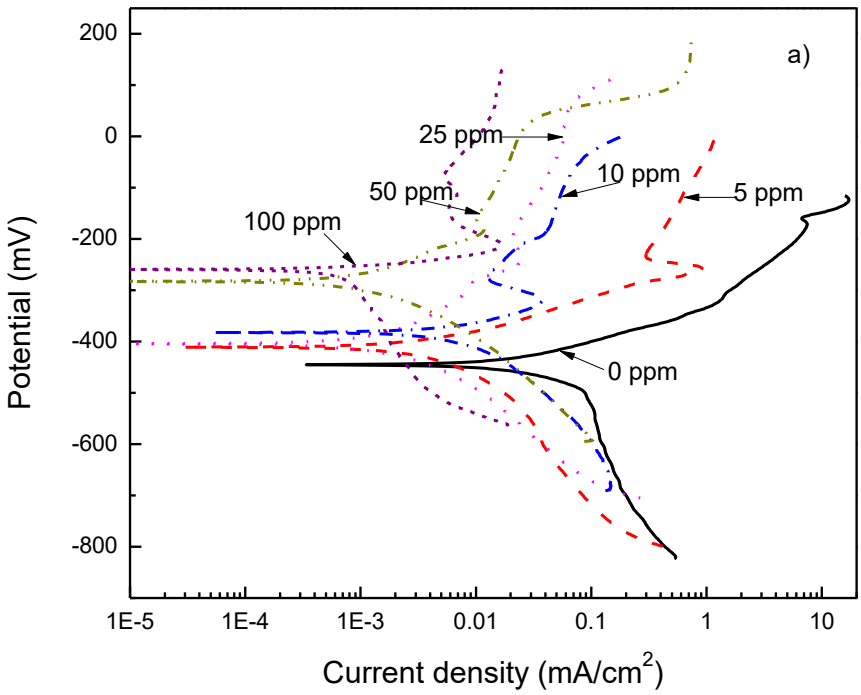

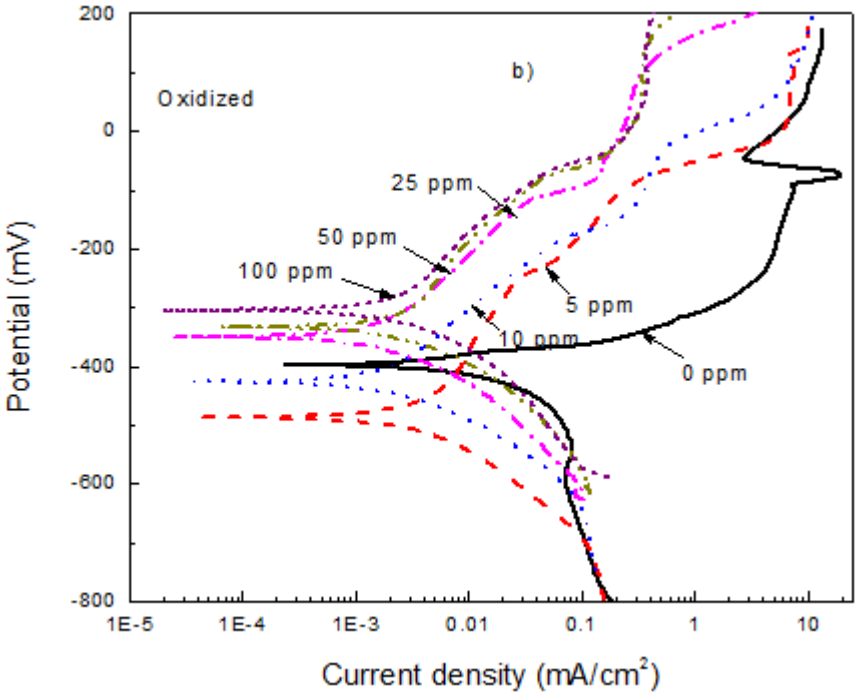

Figure 3. Effect of N-[2-[(2-hydroxyethyl) amino] ethyl]-amide concentration in the polarization curves in 3.5% NaCl for Cu specimens a) without and b) with pre-oxidizing treatment.

The effect of N-[2-[(2-hydroxyethyl) amino] ethyl]-amide concentration in the polarization curves for Cu without and with pre-oxidation treatment are given in Fig. 3. For specimens without pre-oxidation treatment, Fig. 2 a, there is no evidence of an active-passive behavior in absence of inhibitor, only anodic metal dissolution, whereas in the cathodic branch a limiting current density can be observed which is due to the oxygen reduction reaction. In presence of the inhibitor, all the polarization curves exhibited the presence of a passive zone and decreased the I_{corr} value, except with the addition of 100 ppm, where the I_{corr} value was increased. The E_{corr} value shifts towards nobler values for all inhibitor doses except for 100 ppm, which induced a shift towards more active values.

For pre-oxidized specimens, Fig. 3b, when the anodic polarization starts from the E_{corr} value, a in absence of inhibitor anodic current density value rapidly increases, which is due to the dissolution of Cu. The most likely formed corrosion products can be CuCl, Cu_2O, and/or Cu(OH) film [35] which bring some protection to the metal; the anodic current density reaches its highest level or critical value, and a dramatic lowering in its value can be seen beyond this point with the formation of a passive zone at a potential value of -50 mV. The wideness of this passive is very narrow, around -30 mV, observing a trans passive zone due to the dissolution of the passive film. Specimens without pre-oxidation treatment exhibited lower anodic current density values than those obtained for pre-oxidized specimens. On the other hand, a limiting current density value can be seen on the cathodic branch, due to the oxygen reduction reaction at a potential value of -800 mV, whereas the hydrogen evolution reaction is observed for potential values lower than -800 mV. Once the inhibitor addition starts, the E_{corr} value is shifted towards more active values with small doses of inhibitor, i.e. 5 and 10 ppm or towards nobler values for inhibitor concentrations higher than 25 ppm. Additionally, a decrease in the both corrosion and passivation current density values is observed, reaching its lowest value when 100

ppm of inhibitor were added and the passive zone is achieved at a potential value much lower with the addition of fatty amide. Thus, it can be said that an improvement in the passive film properties are achieved by pre-oxidizing. When the inhibitor was added, there is no presence of a limit current density on the cathodic branch.

Obtained electrochemical parameters obtained from polarization curves are given in tables 1 and 2. It can be seen that the I_{corr} values for pre-oxidized specimens were lower than those without pre-oxidation treatment, indicating its beneficial effect on the corrosion protection. In fact, in the case of specimens without pre-oxidizing treatment, the I_{corr} value decreases with an increase in the inhibitor concentration, reaching its lowest value at 100 ppm, whereas the highest inhibitor efficiency value, 95%, was obtained with the addition of 100 ppm, similar to that observed for pre-oxidized specimens. The area covered by the inhibitor, θ, reaches its highest value with inhibitor concentrations of 100 ppm for specimens without and with pre-oxidizing treatment. Thus, although the efficiency values were not affected by pre-oxidizing treatment, the absolute values of the I_{corr} values were decreased. However, in both cases, inhibitor affected anodic and cathodic Tafel slopes, although the cathodic one was more affected. Thus, it can be concluded that N-[2-[(2-hydroxyethyl) amino] ethyl]-amide acts as a mixed type of inhibitor.

Table 1. Electrochemical parameters obtained from polarization curves for Cu specimens without pre-oxidizing treatment.

C_{inh} (ppm)	E_{corr} (mV)	β_a (mV /Dec)	β_c (mV /Dec)	I_{corr} (mA/cm^2)	I.E. (%)	θ
0	-450	65	-385	0.07	----	---
5	-415	60	-305	0.01	85	0.85
10	-400	114	-205	0.008	88	0.88
25	-380	65	-310	0.006	91	0.91
50	-285	65	-190	0.004	94	0.94
100	-560	15	-305	0.002	95	0.95

Table 2. Electrochemical parameters obtained from polarization curves for Cu specimens with pre-oxidizing treatment.

C_{inh} (ppm)	E_{corr} (mV)	β_a (mV /Dec)	β_c (mV /Dec)	I_{corr} (mA/cm^2)	I.E. (%)	θ
0	-398	40	-355	0.0367	----	---
5	-488	164	-152	0.005	86	0.86
10	-424	142	-128	0.0032	91	0.91
25	-350	146	-148	0.0025	93	0.93
50	-336	105	-170	0.0020	94	0.94
100	-304	102	-142	0.0010	95	0.95

Table 3. Inhibitor efficiency and R_p values obtained from the PLR measurements for Cu specimens without and with pre-oxidizing treatment.

C_{inh} (ppm)	R_p value after 24 hours (ohm cm^2)		I.E. value after 24 hours	
	Without pre-oxidizing treatment	Pre-oxidized	Without pre-oxidizing treatment	With pre-oxidizing treatment
0	2,387	3,200	--	--
5	12,207	20,172	80	84.2
10	8,131	12,803	70.6	69.1
25	7,800	15,600	69.3	79.4
50	7,167	15,900	66.7	80.1
100	9,303	23,351	74.3	86.7

3.4 LPR measurements

The effect of N-[2-[(2-hydroxyethyl) amino] ethyl]-amide concentration in the polarization resistance value, R_p, for Cu without and with pre-oxidation treatment are given is shown in Fig. 4 and table 3. It can be seen that for specimens without pre-oxidation treatment, Fig. 4 a, the lowest R_p value is for the uninhibited solution, showing a value which remained more or less constant through the test, lower than 2000 ohm cm^2 cm^2, indicating that the formed corrosion products are not protective. As soon as the inhibitor is added, the R_p value starts to increase, indicating the protective nature of the formed corrosion products. With 5 ppm of inhibitor, the R_p increases continuously up to 12, 000 ohm cm^2, almost one order of magnitude higher than that obtained for the uninhibited solution.

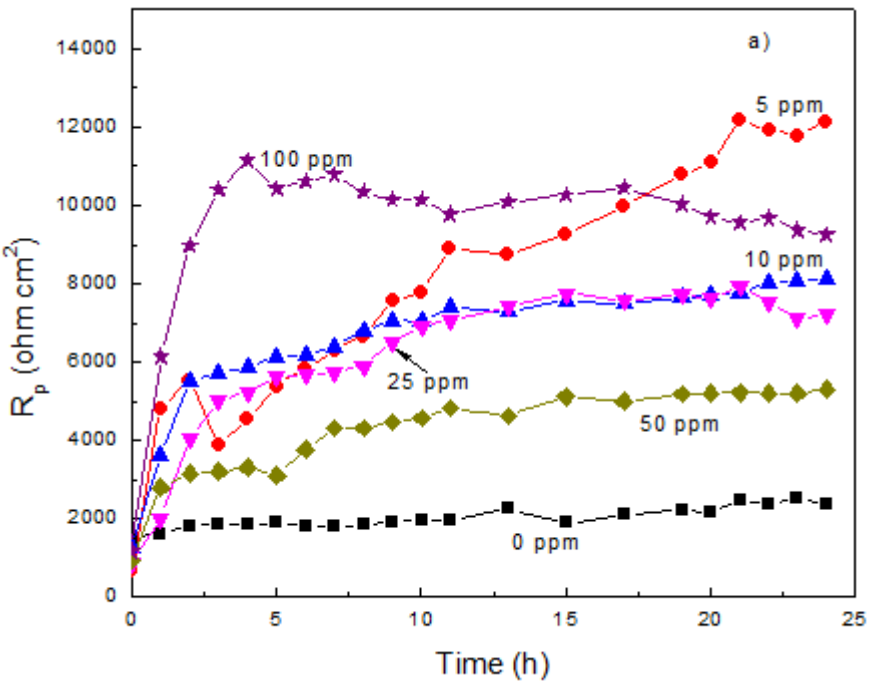

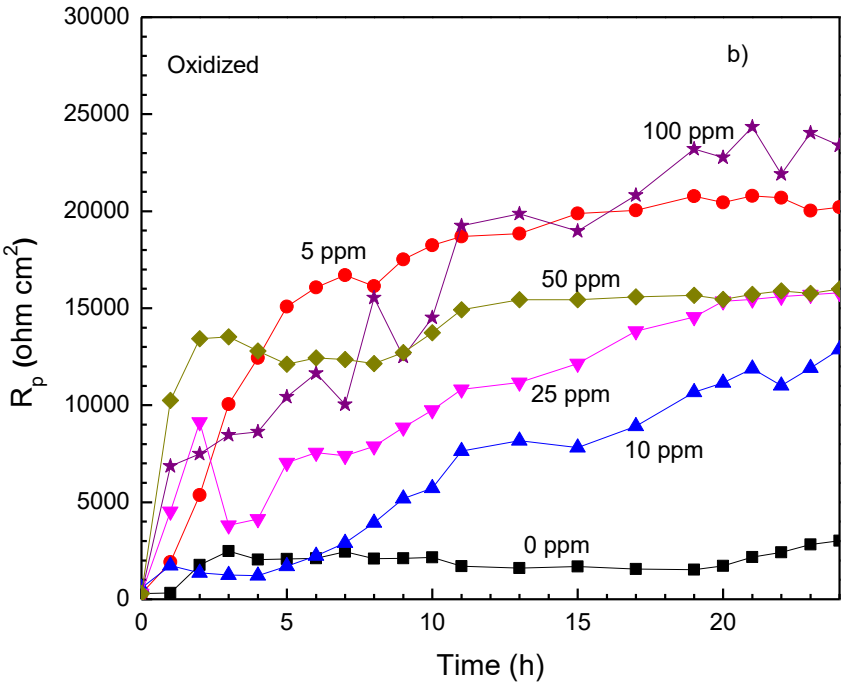

Figure 4. Effect of N-[2-[(2-hydroxyethyl) amino] ethyl]-amide concentration in the variation of the R_p value with time in 3.% NaCl for Cu specimens a) without and b) with pre-oxidizing treatment.

This monotonic increase in the R_p value with time, indicates the protective nature of the corrosion products formed on top of the metal surface. For concentrations higher than 5 ppm, the R_p value increases monotonically as time elapses, indicating an adsorption of the inhibitor onto the metal surface, but the obtained values were lower than those obtained with 5 ppm. The increase in the inhibitor efficiency with increasing the inhibitor concentration can be interpreted on the basis that the adsorption amount and the coverage of inhibitor molecules increases with increasing the testing time [36]. According to table 1, the metal surface area covered by the inhibitor, θ, increased with an increase in both testing time and the inhibitor concentration up to 100 ppm. On the other side, when 100 ppm of N-[2-[(2-hydroxyethyl) amino] ethyl]-amide were added, the R_p value increased rapidly, reaching similar values to those obtained with the addition of 5 ppm but more rapidly, and remained more or less constant throughout the test.

On the other hand, for pre-oxidized specimens, Fig. 4 b, the R_p values for uninhibited solution were slightly higher than those obtained for specimen without pre-oxidation treatment, around 3000 ohm cm^2, indicating the protective nature of oxide preformed. Once again, the highest R_p values were obtained with the addition of 5 ppm, as reported for specimens without pre-oxidizing treatment.

However, with the addition of 100 ppm, similar R_p values to those obtained with 5 ppm were found. Data shown in table 3 indicates that, in general terms the obtained values for pre-oxidized specimens were higher than those obtained without pre-oxidizing treatment, due to the existence of protective formed oxide.

3.5 EIS measurments

The effect of N-[2-[(2-hydroxyethyl) amino] ethyl]-amide concentration in the Nyquist diagrams for Cu in3.5% NaCl solution in the different conditions are given in Fig. 5.

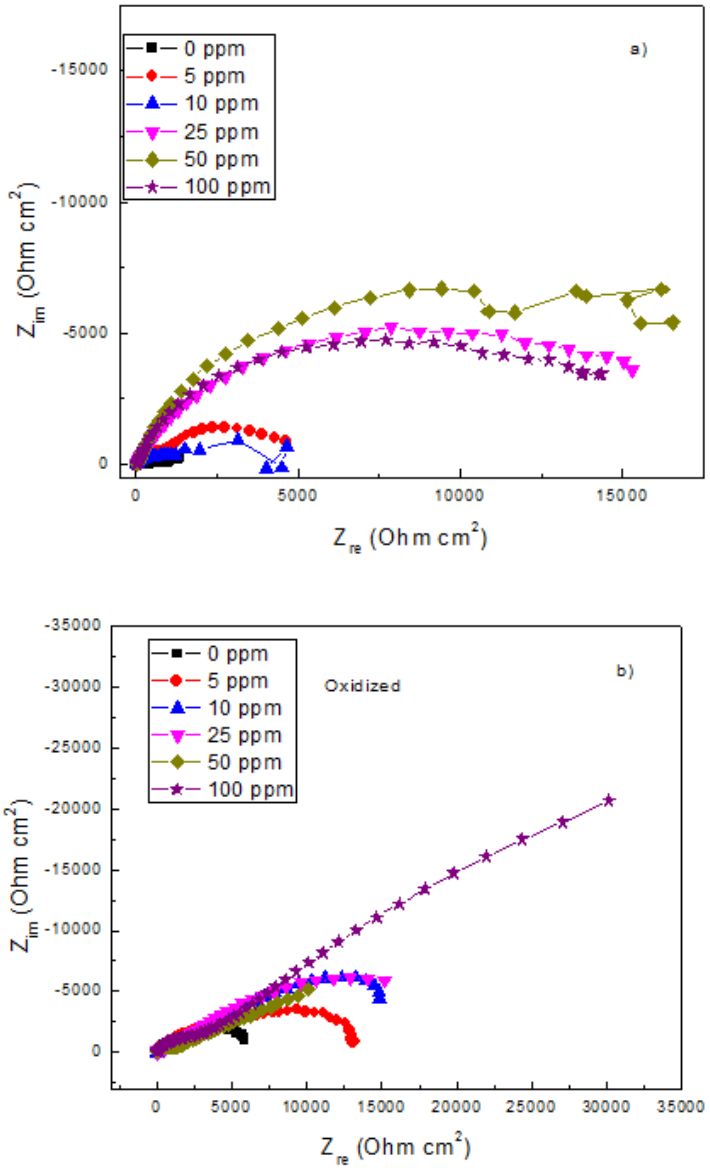

Figure 5. Effect of N-[2-[(2-hydroxyethyl) amino] ethyl]-amide concentration in the Nyquist diagrams in 3.% NaCl for Cu specimens a) without and b) with pre-oxidizing treatment.

Specimens without pre-oxidizing treatment, Fig. 5 a, data describe a single depressed, capacitive semicircle with its center at the real axis, indicating a charge transfer controlled process. The shape of the semicircle did not change with the inhibitor concentration, indicating that the corrosion mechanism did not change. The semicircle diameter increased with the inhibitor concentration, reaching its highest value with a concentration of 50 ppm, and it decreased with a further increase in the inhibitor concentration. The increase in the semicircle diameter is due to the adsorption of the inhibitor molecules with an increase in the surface area covered by the inhibitor molecules and the formation of a protective layer [37, 38]. For the as-received specimen, in absence of inhibitor, these corrosion products are CuCl, Cu_2O, and/or Cu(OH) film [36]. When the inhibitor is added, corrosion products in this case includes the complex formed by inhibitor and released Cu^{2+} ions.

Data for pre-oxidized specimens, Fig. 5 b, describe one depressed, capacitive semicircle at high and intermediate frequency values, and a second capacitive semicircle at lower frequencies. The oxidation of copper gives rise to the observed high frequency capacitive semicircle indicating a charge transfer controlled process, whereas the formation of a corrosion products film gives rise to the observed low frequency loop [37, 38]. When inhibitor is added, the shape of the semicircle, thus the corrosion mechanism, did not change, only the real impedance value at the lowest frequency or total impedance, which is the sum of the two semicircles diameter. Corrosion products in this case includes the by pre-formed oxide together with the complex formed inhibitor and released Cu^{2+} ions. Total impedance increased even more for the pre-oxidized specimen in presence of the inhibitor since in this case formed film on top of metal includes the oxide formed during the pre-oxidizing treatment and the complex formed by inhibitor and released Cu^{2+} ions.

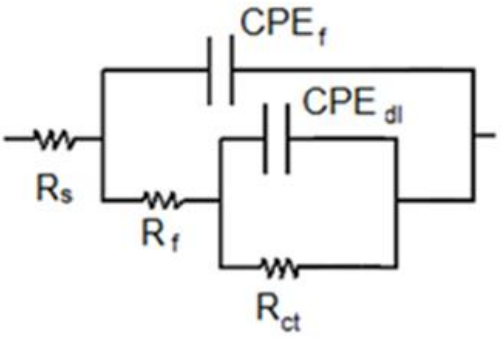

Figure 6. Electric circuit used to simulate EIS data for Cu specimens with and without pre-oxidizing treatment.

EIS data can be analyzed with the help of equivalent electric circuit shown in Fig. 6, and electrochemical parameters such as solution resistance, R_s, the charge transfer resistance, R_{ct}, the film resistance, R_f, the double layer capacitance, C_{ct}, and the film capacitance, C_f, can be calculated. In Fig. 5, the diameter of the high frequency semicircle corresponds to the film resistance, R_f, whereas that for the low frequency semicircle correspond to the charge transfer resistance, R_{ct}. The sum of $R_f + R_{ct}$, gives the polarization resistance, R_p. Since the observed semicircles are depressed, which is due to the inhomogeneity and surface roughness, a constant phase element, CPE, is introduced instead of an

ideal double layer capacitor, C_{dl},. This CPE_{dl} is placed instead of the ideal C_{dl}, and CPE_f introduced instead the ideal capacitance of the film formed by the inhibitor and the corrosion products. To calculated the CPE impedance , following equation is used:

$$Z_{CPE} = Y^{-1} (iw)^{-n} \quad (1)$$

where *Y* is the admittance, i is √-1, *w* is $2\pi f$, *f* the frequency and n is a parameter that gives surface properties such as roughness etc…Electrochemical parameters obtained from the fitting of EIS data by using electric circuits shown in Fig. 6 are given in tables 4 and 5.

Table 4. Electrochemical parameters to simulate EIS data for Cu specimens without pre-oxidizing treatment.

C_{inh} (ppm)	R_s (ohm cm^2)	R_{ct} (ohm cm^2)	C_{dl} ($\mu F\ cm^{-2}$)	n_{dl}	R_f (ohm cm^2)	C_f ($\mu F\ cm^{-2}$)	n_f
0	10.5	1.6×10^3	1.1×10^{-4}	0.66	2.3×10^2	5.9×10^{-3}	0.45
5	11.7	1.5×10^3	2.4×10^{-4}	0.70	3.1×10^3	1.2×10^{-3}	0.72
10	12.6	1.0×10^1	7.7×10^{-4}	0.49	5.4×10^3	7.1×10^{-5}	0.82
25	14.3	1.4×10^1	2.1×10^{-5}	0.48	1.9×10^4	2.5×10^{-5}	0.85
50	10.3	1.3×10^1	8.3×10^{-6}	0.54	2.1×10^4	3.9×10^{-5}	0.88
100	12.8	1.4×10^1	9.9×10^{-6}	053	1.6×10^4	3.1×10^{-5}	0.79

Table 5. Electrochemical parameters to simulate EIS data for Cu specimens without pre-oxidizing treatment.

C_{inh} (ppm)	R_s (ohm cm^2)	R_{ct} (ohm cm^2)	C_{dl} ($\mu F\ cm^{-2}$)	n_{dl}	R_f (ohm cm^2)	C_f ($\mu F\ cm^{-2}$)	n_f
0	12.5	86.6	4.7×10^{-5}	0.76	4950	2.8×10^{-3}	0.56
5	13.8	310	7.7×10^{-6}	0.88	1.25×10^4	7.6×10^{-4}	0.62
10	14.0	320	6.2×10^{-6}	0.89	1.50×10^4	4.4×10^{-4}	0.67
25	12.3	702	5.7×10^{-6}	0.86	2.03×10^4	3.2×10^{-5}	0.76
50	13.3	1320	4.3×10^{-6}	0.88	2.25×10^4	2.3×10^{-5}	0.88
100	9.8	2440	2.9×10^{-6}	096	3.22×10^4	1.21×10^{-5}	0.94

From these tables, it can be seen that for no pre-oxidized and pre-oxidized specimens, the R_f values are higher than those for R_{ct}, indicating that the corrosion resistance is given by the formed film on top of the metal. Secondly, the R_f values for pre-oxidized specimens are higher than those obtained for specimens without pre-oxidizing treatment. This might be the explanation of the low effect of pre-oxidizing on the inhibitor performance. The organic molecules of inhibitors can be adsorbed on the Cu surface both through chemical and physical interactions. In physical adsorption, there is an electrostatic interaction between charge of inhibitor molecules and the charged metal surface, whereas in the chemical adsorption involves the sharing or transfer charge from inhibitor molecule on the charged metal surface to form covalent bond coordination. Chemical adsorption is stronger than a

physical one. Porcayo-Calderon showed that our inhibitor has a chemical type of adsorption on Cu, and this could explain the good performance as a corrosion inhibitor it exhibited [25]. However, when there is an oxide on top of the metal, organic inhibitor molecules must interact with a semiconductor, no with a metal, which is a conductor, therefore it is expected that the type of interaction is weaker than that with a metal. Therefore, the adsorption of the inhibitor with the per-formed oxide must be weaker, physical in nature, than that on top of Cu. Thus, the effect of pre-formed oxide is to act as a physical barrier between metal and the environment as evidenced by the R_f values given above since the adsorption of the inhibitor on the oxide is weak and by data in table 3, where the oxide increased the Rp values by a factor of two only. For instance, in absence of inhibitor, the film resistance value for pre-oxidized specimen was 4950 ohm cm^2, much higher than that obtained for specimen without pre-formed oxide, 230 ohm cm^2. Similarly, the R_f value for a doses of 5 ppm of inhibitor was 3.1×10^3 and 1.25×10^4 ohm cm^2 for specimens without and with pre-oxidizing treatment respectively. On the other side, for both type of specimens, the R_f normally increases whereas the C_f value decreases with an increase in the inhibitor concentration. Finally, a low surface roughness due to a low corrosion rate gives rise to an n_f value close to 1 whereas high roughness of the surface due to a high dissolution rate gives rise to an n_f value close to 0.5. It is clear from tables 3 and 4 that the lowest n_f values for both type of specimens were obtained in absence of inhibitor due to a high surface roughness due to a high dissolution rate. On the contrary, the highest n_f values were obtained at 50 and 100 ppm for specimens without and with pre-oxidizing treatment respectively, where the lowest dissolution rate values were obtained, and thus, the lowest surface roughness.

3.6 Micrographs

Some SEM micrographs of corroded specimens after the LPR experiments are shown in Fig. 7. For specimen without pre-oxidizing treatment and corroded in absence of inhibitor, Fig. 7 a, it can be seen a completely corroded metal surface, where the corrosion products layer covers a very small part of the surface area, and this layer is completely porous, non-adherent, and it has been detached from the metal surface. For pre-oxidized specimen and corroded in absence of inhibitor, Fig. 7 b, the corrosion products layer covers a bigger surface area as compared to the specimen without pre-oxidizing treatment, however, the underlying metal surface still suffers from some type of corrosion, which indicates that this layer provides a limited corrosion protection to the metal.

For specimen without pre-oxidising treatment and corroded in presence of 5 ppm of N-[2-[(2-hydroxyethyl) amino] ethyl]-amide, Fig. 7 c, the corrosion products are more compact, without evidence of porous or micro cracks, but that it has been detached from the metal surface, leaving unprotected some parts of the metal.

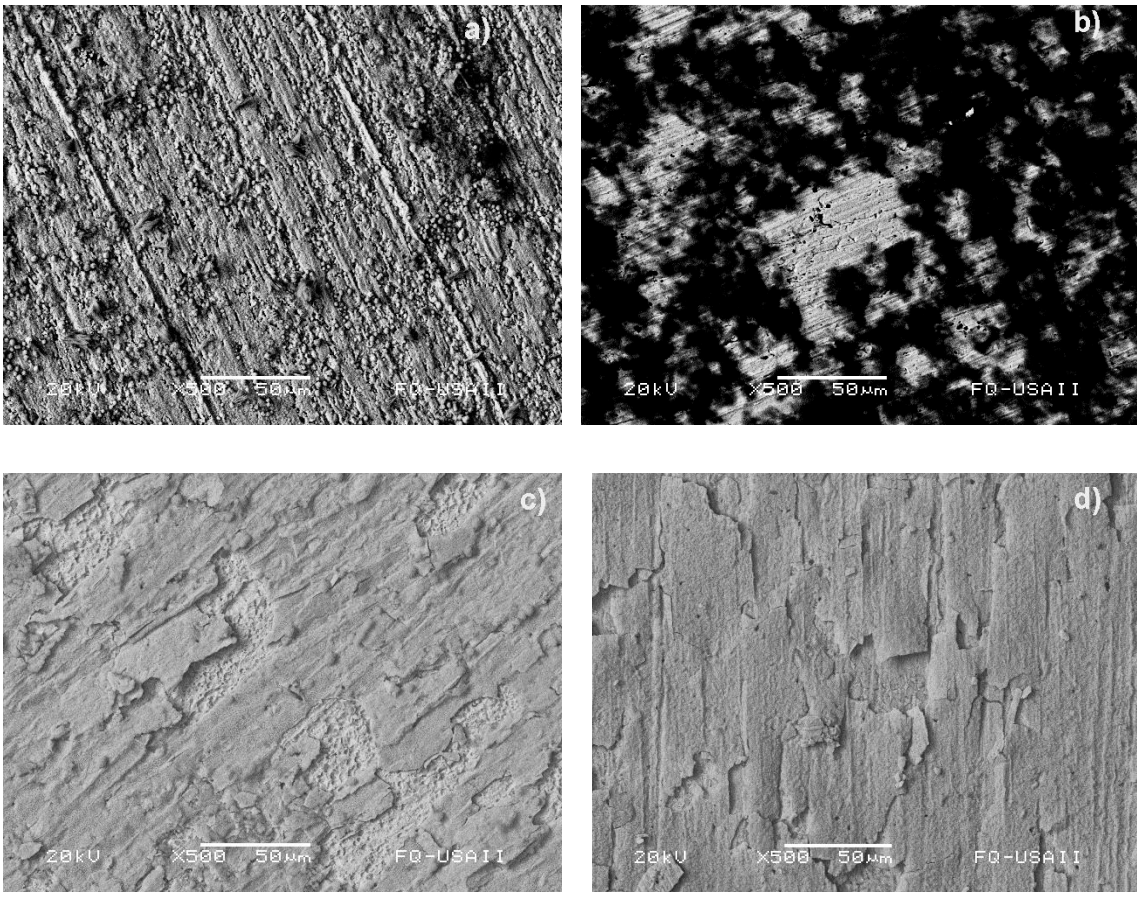

Figure 7. SEM micrographs of Cu specimens a) and c) without pre-oxidizing treatment and b) and d) with pre-oxidizing treatment corroded in 3.5% NaCl containing 0 ppm, a) and b), and 5 ppm , c) and d) of N-[2-[(2-hydroxyethyl) amino] ethyl]-amide.

The unprotected parts of the underlying metal show evidence of some kind of corrosion attack. For specimen with pre-oxidizing treatment and corroded in presence of 5 ppm of N-[2-[(2-hydroxyethyl) amino] ethyl]-amide, Fig. 7 d, the corrosion products layer is very compact and covers almost completely the metal surface, decreasing, thus, the alloy corrosion rate as reported by the electrochemical results above. By comparing Figs. 7 a and b, which were corroded at the same inhibitor concentration, i.e. 5 ppm, it is evident the beneficial effect of pre-oxidizing in the adherence of the formed corrosion products layer, and, thus, in the corrosion protection given by the addition of N-[2-[(2-hydroxyethyl) amino] ethyl]-amide.

4. CONCLUSIONS

The effect of plasma pre-oxidizing on the performance of of N-[2-[(2-hydroxyethyl) amino] ethyl]-amide as corrosion inhibitor for Cu in 3.5% NaCl has been studied. Polarization curves have shown that corrosion rate was decreased and the passive film properties were improved, since the I_{corr} and I_{pass} values were decreased by pre-oxidizing treatment. LPR results showed that regardless of the pre-oxidizing treatment, the optimum inhibitor concentration was 100 ppm. Corrosion protection given

by the inhibitor and pre-oxidizing treatment improves as time elapses due to an increase of the surface area covered by the corrosion products layer. By pre-oxidizing, the adherence of the inhibitor-formed film to the metal is improved.

References

1. H. Ma, S. Chen L. Niu, S. Zhao, S. Li, and D. Li, *J. App. Electrochem*., 32 (2002) 65.
2. K.F. Khaled, *Mat. Chem. Phys.*, 112 (2008) 104.
3. H. Bi, G.T. Burstein, B.B. Rodriguez and G. Kawaley, *Corros. Sci*., 102 (2016) 510.
4. P. Yu, D. M. Liao, Y. B. Luo and Z. G. Chen, *Corrosion*, 59 (2003) 314.
5. El-Sayed M. Sherif and Abdulhakim A. Almajid, *J. Appl. Electrochem*., 40 (2010) 1555.
6. M. M. Antonijevic and M. B. Petrovic, *Int. J. Electrochem. Sci.*, 3 (2008) 1.
7. B. Hammouti, A. Dafali, R. Touzani and M. Bouachrine, *J. Saudi Chemical Society*, 16 (2012) 413.
8. A. Yabuki and M. Murakami, *Corrosion*, 63 (2007) 249.
9. E. Stupnisek-Lisac, A.Brnada and A.D.Mance, *Corros. Sci*., 42 (2000) 243.
10. Maryam Ehteshamzadeh, T. Shahrabi and M. Hosseini, *Anti-Corr. Meth. Mat*., 53 (2006) 296.
11. Maryam Ehteshamzade, T. Shahrabi and M.G. Hosseini, *Appl. Surf. Sci*., 252 (2006) 2949.
12. A.A. El Warraky, *Anti-Corr. Meth. Mat*, 50 (2003) 40.
13. J.B. Matos, L.P.Pereira, S.M.L.Agostinho, O.E.Barcia, G.G.O. Cordeiro and E.D'Elia, *J. Electroanal. Chem*., 570 (2004) 91.
14. H. Otmacic, J. Telegdi, K. Papp and E. Stupnisek-Lisac, *J. Appl. Electrochem*., 34 (2004) 545.
15. Carmel B. Breslin and D.D. Macdonald, *Electrochim. Acta*, 44 (1998) 643.
16. K.F. Khaled and N. Hackerman, *Electrochim. Acta*, 49 (2004) 485.
17. C. Wang, S. Chen and S. Zhao, J. Electrochem. Soc.,151 (2004) B11.
18. M. Kendig and S. Jeanjaquet, J. Electrochem. Soc., 149 (2002) B47.
19. D.Q. Zhang, L.X. Gao and G.D. Zhou, *Appl. Surf. Sci.*, 225 (2004) 287.
20. A.G. Christy, A. Lowe, V. Otieno-Alego, M. Stoll and R.D. Webster, *J. Appl. Electrochem.*, 34 (2004) 225.
21. G. Ji, S. Anjum, S. Sundaram and R. Prakash, *Corros. Sci.*, 90 (2015) 107.
22. S. K. Shukla, P. Dwivedi, S. Sundaram, E. E. Ebenso and R. Prakash, *Int. J. Electrochem. Sci*., 7 (2012) 12146.
23. M. Ramananda Singh, *J. Mater. Environ. Sci.*, 4 (2013) 117.
24. X. Liu, P.C. Okafor and Y.F. Zheng, *Corros. Sci*., 51 (2009) 744.
25. J. Porcayo-Calderon, L.M. Martínez de la Escalera, J. Canto and M. Casales-Diaz, *Int. J. Electrochem. Sci.*, 10 (2015) 3160 .
26. Fengjie Yan, Xuegang Wang, Xiaoming Wang, Xingeng Li and Chengguo Wang, *Int. J. Electrochem. Sci.*, 12 (2017) 11212.
27. Mineaki Matsumoto, Takeharu Kato, Kazuyuki Hayakawa, Norio Yamaguchi, Satoshi Kitaoka and Hideaki Matsubara, *Surface and Coatings Technology* 202 (2008) 2743.
28. Fujio Abe, H. Kutsumi, H. Haruyama and H. Okubo, *Corros. Sci.* 114 (2017) 1.
29. E. Boztepe, A.C. Alves, E. Ariza, L.A. Rocha, N. Cansever and F. Toptan *Surface and Coatings Technology,* 334 (2018) 116.
30. J. Alphonsa, V.S. Raja and S. Mukherjee, *Corros. Sci*., 100 (2015) 121.
31. M. Benmessaoud, K. Es-salah, N. Hajjaji, H. Takenouti, A. Srhiri and M. Ebentouhami, *Corros. Sci.*, 49 (2007) 3880.
32. L. Bousselmi, C. Fiaud, B. Tribollet and E. Triki, *Electrochim. Acta*, 44 (1999) 4357.
33. C.W. Yeow and D.B. Hibbert, *J. Electrochem. Soc*., 130 (1983) 786.
34. H. Ma, S. Chen, L. Niu, S. Zhao, S. Li, and D. Li, *J. Appl. Electrochem*., 32(2002) 65.

35. M. Benmessaoud, K. Es-salah, N. Hajjaji, N. Takenouti and M. Ebentouhami, *Corros. Sci.*, 49(2007) 3880.
36. Huan-huan Zhang, Xiaolu Pang, Meng Zhou, Chao Liu, Liang Wei and Kewei Gao, *Appl. Surf. Sci*. 356 (2015) 63.